Geologica Acta, Vol.2, Nº4, 2004, 321-331
Available online at www.geologica-acta.com

geologica acta

Estimating paleogeographic, hydrological and climatic conditions in the upper Burdigalian Vallès-Penedès basin (Catalunya, Spain)

K. BITZER

Universität Bayreuth. Abteilung Geologie
Universitätsstr. 30. D-95440 Bayreuth, Germany. E-mail: klaus.bitzer@uni-bayreuth.de

ABSTRACT

During the evolution of the Vallès-Penedès basin, several transgressive pulses in the upper Burdigalian led to a partial flooding of the western part of the basin, leaving locally sabkha-salina evaporite sediments in the area of the village of Vilobí. Due to its geometric configuration with a restricted access to the open sea, deeper marine evaporites do not occur in the basin. A mathematical model of fluid circulation, evaporation outflow, solute transport and evaporite deposition is applied in order to test possible paleogeographic, hydrological and climatic conditions which may have influenced salinity of sea water in the upper Burdigalian Vallès-Penedès embayment. Simulation results indicate that the absence of marine gypsum sediments in the basin may be related to a significant freshwater supply. The shift from the Neogene basin drainage pattern along the complete basin axis with elevated freshwater discharge to the river drainage towards the Barcelona area occurred at later stages of the basin evolution.

KEYWORDS | **Vallès-Penedès half-graben. NW Mediterranean. Vilobí sequence. Evaporites. Sedimentation. Simulation. Evaporation outflow.**

INTRODUCTION

The Vallès-Penedès basin is a NW-striking Neogene halfgraben with 100 km elongation and 12 to 14 km width located at the continental margin of the Valencian Gulf (Fig. 1). Its geologic evolution is characterized by tectonic subsidence and continental and marine sedimentation. The thickness of the Neogene sediment fill reaches up to 4000 m. An initial rifting phase during upper Oligocene and lower Miocene in the context of the opening of the Valencian Gulf caused block-faulting with narrow horst and graben structures along the continental margin. The rifting stage was followed by thermal subsidence during upper Burdigalian time. As a result of its tectonic and sedimentary evolution, the basin exhibits a heterogeneous sediment fill with continental clastics, marine deposits including reef buildups and sabka-salina evaporite sediments. Detailed descriptions and interpretations of the evolution of the Catalan margin, the structural setting and sedimentary filling of the Vallès-Penedès basin are given by Cabrera et al. (1991), Guimerà et al. (1992) and Roca et al. (1999). In this contribution, a simulation model of flow circulation, evaporation process and evaporite sedimentation is applied to the upper Burdigalian basin configuration.

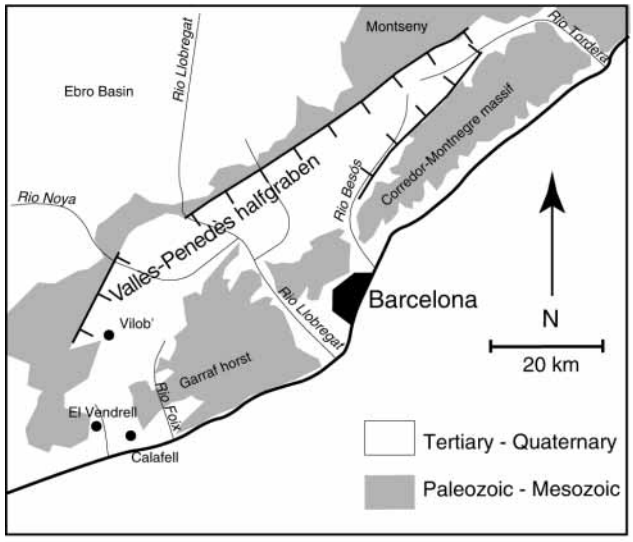

FIGURE 1 | **Simplified geologic map and fluvial system in the Vallès-Penedès half-graben.**

Late Burdigalian evaporites in the Vallès-Penedès basin have been mined in gypsum-quarries at the village of Vilobí, about 6 km north of Vilafranca del Penedès. The formation of the Vilobí-gypsum deposits, called Vilobí-sequence (Cabrera et al., 1991) is attributed to a transgressive-regressive event during the upper Burdigalian time. Its petrographic characteristics have been studied by Ortí and Pueyo (1976). Upper Burdigalian evaporites in the Vallès-Penedès basin are known only from the location of Vilobí and the lateral continuity of the deposit is uncertain.

Petrographic and sedimentological characteristics of the Vilobí sequence point to sedimentation processes in a coastal sabkha-saline. Although the geometry of the Penedès basin shows an elongated embayment with restricted connection to open sea (Fig. 2), marine evaporite sedimentation in the basin apparently did not take place after deposition of the Vilobí sequence. The objective of this contribution is to estimate paleogeographic, hydrological and climatic conditions during the transgressive flooding of the basin after deposition of the Vilobí sequence. A simplified mathematical model is applied, which simulates the processes of sea water flow in the upper Burdigalian embayment of the Vallès-Penedès basin, possible freshwater inflow and evaporation outflow. Simulation runs are carried out with the SIMSAFADIM code (Bitzer and Salas, 2002), which is an integrated fluid flow, transport and sedimentation model including a simplified evaporite deposition approach. In its current version the program takes into account the three-dimensional geometry of the basin, changes in water depth due to sedimentation and sea level changes, thus incorporating some aspects of the heterogeneity of an evolving evaporite basin. Although the model assumes various simplifications as for example the absence of density driven fluid circulation, absence of brine reflux and the restriction to only three evaporite sediment types, it represents a useful tool to test hypotheses on the evolution of an evaporite basin.

SEDIMENTARY COLUMN AT THE VILOBÍ OUTCROP

The Vilobí Gypsum deposit has a thickness of about 60 m. It rests upon 5 m of continental Tertiary shales, carbonates and marls, and is overlain by red nonmarine clays. These Tertiary sediments are separated by an erosional unconformity from the underlying Cretaceous carbonate rocks. The Vilobí sequence can be divided into 4 units (Fig. 3). Units 1 to 3 are composed of secondary gypsum (coming from the hydration of precursor anhydrite), and unit 4 at the top remains as primary gypsum (Ortí and Pueyo, 1976; Ortí, 1990). The lowermost gypsum unit (unit 1), with a thickness of about 28 m, is characterized by laminated to nodular and enterolithic gypsum lithfacies. Unit 2, of about 28 m thickness, is composed of radial aggregates of gypsum and unit 3, of about 8 m thickness, is comprised of lenticular megacrystals of gypsum. Both the radial aggregates and the lenticular megacrystals are diagenetic gypsum textures, overprinted on the original laminated to nodular lithofacies. Unit 4 has a laminated lithofacies composed of microcrystalline and microselenitic gypsum.

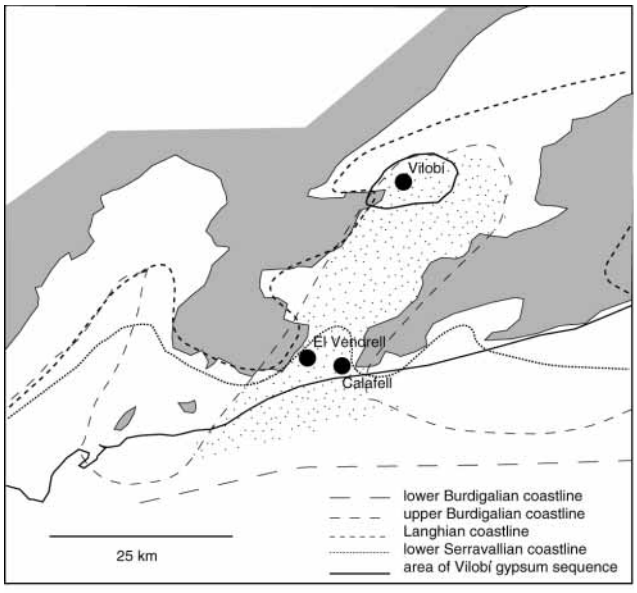

FIGURE 2 | **Paleogeographic configuration of the Vallès-Penedès half-graben from the Burdigalian until early Serravallian time (adapted from Guimerà et al., 1992). The dotted area, bounded by the upper Burdigalian coastline, corresponds to the modeled zone of the basin.**

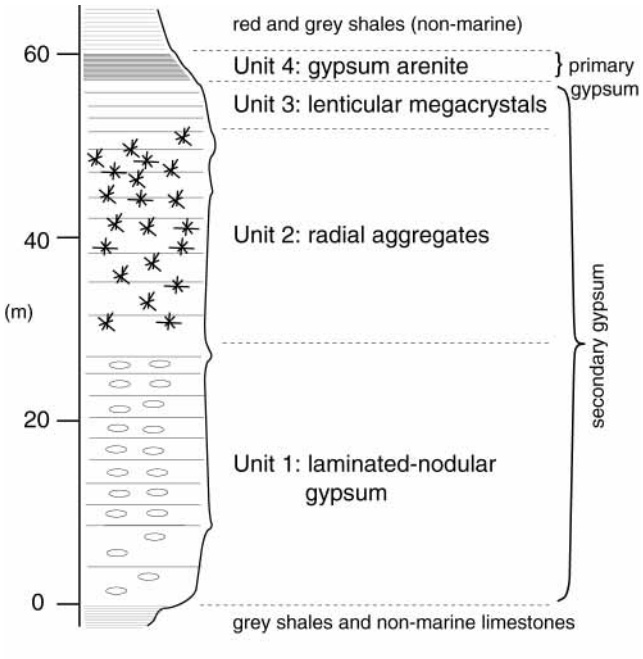

FIGURE 3| **Sedimentary sequence at Vilobí (adapted from Ortí and Pueyo, 1976).**

All units precipitated initially as laminated gypsum in a shallow salina. During sedimentation of units 1 to 3, continuous fluctuations of water level resulted in the sabkhatization of the salina and the gypsum transformation into (nodular and enterolithic) anhydrite. At the top of unit 3 sedimentological conditions changed, involving an erosional surface. Upon this surface, gypsum layers of unit 4 accumulated and remained diagenetically unchanged. Rehydration of anhydrite in units 1 to 3 into secondary gypsum and the formation of the erosional surface are most probably related to the same process or event.

Although the Vilobí Gypsum deposit is interlayered between non-marine sediments, the isotopic composition of the sulphates indicates that the precipitating brines were of marine origin. Thus, this deposit has been interpreted as a coastal sabkha-salina being fed by seawater and with permanent outflow of heavy brines towards the sea (Ortí, 1990).

PALEOGEOGRAPHIC EVOLUTION OF THE BASIN DURING BURDIGALIAN AND LANGHIAN TIME

Rifting during lower Burdigalian time with rapidly subsiding blocks along normal faults led to a strong compartimentalization of the sedimentary environment with fluvial deposits, alluvial fan deposits and playa-type sediments (Cabrera, 1981, 1982). Marine ingressions apparently did not occur during this phase. In the following phase of thermal subsidence during upper Burdigalian time, transgressive pulsations caused a progressive flooding from the Valencian Gulf northward, covering previously continental areas and leaving evaporite sediments in a saline at the northwestern shoreline at Vilobí (Fig. 2). The extension of the upper Burdigalian embayment probably continues some kilometers towards northeastern direction (Cabera et al., 1991; Guimerà et al., 1992) and possibly ends in an estuarine river mouth. At this moment, the paleogeograhic situation was characterised by a near mountain range in the north, which was separated from the subsiding basin by the principal normal fault. This area is thought to be the principal source of terrigenous sediments, which were transported towards the basin center by small rivers and alluvials fans. On the southeastern shore, the Garraf block locks the embayment from the open sea, leaving only a small connection to the open sea in the area between El Vendrell and Calafell. The Vallès-Penedès basin formed a depression which probably extends towards northeast with a river system, which drained a considerable area. However, details of the ancient river system are not known. It is difficult to conceive from the paleogeographic configuration, that the current Llobregat system at that moment drained towards the Barcelona area. Water depths in the embayment have probably been shallow due to the proximity of sediment sources and the initial state of flooding. Accomodation space created by thermal subsidence was probably rapidly consumed by sedimentation.

During Langhian time, transgressive pulsations and continued thermal subsidence caused a generalized flooding with coastlines moving considerably towards northeast. At that moment, the Garraf block got almost completely flooded. As a result of the changing paleogeographic situation, carbonate sedimentation with small coral reefs formed on the margin of the Garraf block while terrigenous input from the northern mountain range was accumulated in the central parts of the basin. Sedimentation processes and the interaction between carbonate and clastic sedimentation in the Vallès-Penedès basin during the Langhian have recently been modeled by Gratacós et al. (2003). During lower Serravallian time, most parts of the basin were exposed above sea level, except for a small area between El Vendrell and Calafell. The marine episode in the basin was finished by the end of lower Serravallian time

PRECIPITATION OF EVAPORITES FROM SEAWATER

The chemical evolution of evaporite sediments is considered as a sequential precipitation from seawater according to the degree of saturation of various salts (Eugster and Hardie, 1978). To some minor degrees, ion

exchange processes may affect the chemical evolution, however, the specific ion capacity of clay in saline brines is low in comparison to the ions within the brine. Sulfate-sulfide redox reactions may have some importance at freshwater/saline water boundaries (Custodio et al., 1987). The dominating process, however, is the chemical evolution of the saline brine during evaporation of seawater. Quantitative models of brine evolution have been applied to several evaporite sequences, such as for the Eocene Catalan potash basin (Ayora et al., 1994), where the chemical evolution was compared to chemical compositions in fluid inclusions. Most models, such as the model published by Risacher and Clement (2001), are based on the Pitzer interaction model for calculation of chemical evolution of brines, allowing for open (meaning that precipitated salts may not be dissolved subsequently) and closed systems. The Pitzer model has the advantage that chemical processes may be calculated at high ionic strength and calculated solubilities are similar to experimental data. Geochemical calculations of brine evolution based on the Debye-Hückel model, for example, excessively overestimate gypsum solubilities in relation to halite at higher brine concentrations (Bethke, 1996).

Solubility of gypsum is controlled by the concentration of other ions. Due to the dominance of sodium and chloride ions in marine water, the dependence of gypsum solubility from these ions is of primary importance (e.g. James, 1992). Maximum solubility of gypsum in destilled water is at 2.08 g/kg water. At an average concentration of 35 g sea salt per kg sea water, measured $CaSO_4$ concentrations are in the order of 1.1 g/kg water (James, 1992) and rise linearly with increasing concentration due to evaporation. Figure 4 compares maximum solubility of gypsum with regard to sea salt concentration from experimental data taken from James (1992, p 49) and solubilities calculated using the PHREEQ-C code. The diagram reflects the concentration increase induced induced by evaporation of sea water and the change of solubility of gypsum in relation to sea salt concentration. It further illustrates the fact that calculated solubilities based on the Debye-Hückel model considerably overestimate gypsum solubilities, as stated before. Up to a sea salt concentration of about 110 g/kg water, $CaSO_4$ concentrations in the brine remain below maximum solubility, and no precipitation takes place. At that value, $CaSO_4$ concentration in the brine starts to exceed maximum solubility at 4.1 g/kg water and and precipitation starts. As sea salt concentration continues to rise if evaporation outflow continues, maximum solubility of $CaSO_4$ decreases and precipitation therefore accelerates. Other ions change the solubility of $CaSO_4$ in various ways, and the geochemical processes are considerably more complicated. However, for the purpose of calculating gypsum precipitation from normal sea water, Voigt (1990) suggests, that it is sufficient to consider the dependence of gypsum precipitation in relation with the main sea salt, which is halite (Table 1). As a first approximation, the SIMSAFADIM model incorporates the experimental gypsum solubilities from James (1992). This simplification is acceptable if halite does not precipitate and [Ca] and [SO_4] are not present in the continental water, so that [Ca] and [SO_4] are only due to sea water evaporation.

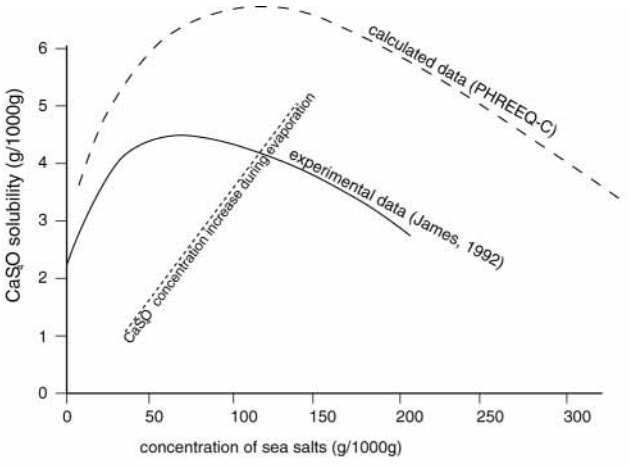

FIGURE 4 | **Solubility of gypsum in relation to concentration of sea salts and gypsum concentration increase during evaporation (from James, 1992).**

EVAPORATION OF SEAWATER

Assuming that the chemical evolution of salts from a brine is a consequence of sequencial precipitation according to the degree of saturation of various salts at constant salt mass, the key process for the formation of evaporite sediments is the evaporation of sea water. Evaporation outflow expresses the difference between precipitation of rain water to the sea and evaporation of

TABLE 1 | **Concentration of main components in sea waterwith 35‰ salinity (from Turekian, 1985).**

Main component	g/kg
Chloride	19.353
Sodium	10.76
Sulphate	2.712
Magnesium	1.294
Calcium	0.413
Potassium	0.387
Bicarbonate	0.142
Bromide	0.067
Strontium	0.008
Bor	0.004
Fluoride	0.001

sea water and may be given in m/y. Evaporation outflow is primarily a function of heat balance, water activity and climatic conditions (Dietrich, 1959). For the area of the Arabian Gulf at Abu Dhabi, measured evaporation outflow is in the order of 1.24 m/y (Alsharhan and Kendall, 2003) and for the western Mediterranean Sea, an evaporation outflow of 1 m has been estimated. While rainfall at the Abu Dhabi area is extremely low in the order of 40 mm/y, the western Mediterranean Sea shows strong seasonal variations with maximum rainfall rates in the order of 200 mm/y. In general, a maximum of evaporation outflow of 1.2 m/y is measured at latitudes of 30° north and can be recognized in elevated salinities of surface sea water (Tolmazin, 1985). Salinity in ocean waters at 30° northern latitude rises up to 37‰, while ocean water at lower latitudes shows normal salinities at 35 ‰ due to negative evaporation outflow (rainfall exceeding evaporation). Evaporation also depends on the salinity of the evaporating brine. Extremely concentrated brines at the Dead Sea have shown almost zero evaporation (Yechieli and Wood, 2002). This is due to the fact that extremely concentrated brines offer almost no free water molecules for evaporation, a process which is considered by the SIMSAFADIM model by assuming a linear relationship between evaporation outflow and brine concentration. Another limiting factor is relative humidity, which requires values less than 76% in order to produce brines from which halite can precipitate (Kinsman, 1976).

Evaporation does not only govern the chemical evolution of brines and the precipitation process of evaporites, it also affects the circulation of water in the oceans. Due to elevated water densities from differences in evaporation of sea water and precipitation of rain, deep thermohaline circulation patterns evolve, as for example in the Gibraltar Straight with Atlantic shallow water at normal salinity flowing into the Mediterranean Sea and higher saline water returning at greater depth towards the Atlantic Ocean. In the case of the Arabian Gulf, a counterclockwise thermohaline circulation pattern has been observed. At temperatures between 0 and 50° C and generally strong winds, a strong evaporation outflow in the order of 1.24 m/y and annual precipitaction of less than 40 mm, sea water enters the Arabian Gulf at the straight of Hormuz with salinities of 37‰ at shallow depth. At greater water depth, a brine with a concentration of 40‰ leaves the Arabian Gulf. Salinity at the Abu Dhabi coast reaches 70‰ (Alsharhan and Kendall, 2003). Such values, however, are not sufficient to provide precipitation of any evaporite sediment. The local configuration of the coastal area (water depth, connection to open sea, etc.) needs therefore to be known in order to evaluate the potential for evaporite sedimentation.

Circulation of water masses in shallow evaporite basins will also be influenced by atmospheric processes, inflow of freshwater at river mouths and from the extent of evaporation outflow and its compensation from inflowing sea water from the open sea. When the basin is completely separated from the open ocean, evaporation outflow no longer affects the circulation pattern and recharge of salts has terminated.

Density driven circulation and reflux of brines towards open sea strongly controls the evolution of an evaporite basin, as it continuously removes the more soluble salts from the basin and allows the less soluble minerals to accumulate. This process, however, is not included in the calculations presented here. As brine reflux is not incorporated, calculation of halite sedimentation using the SIMSAFADIM code would considerably overestimate halite precipitation and underestimate solubility of gypsum.

MODELING APPROACH

Simulation of evaporite sedimentation was among the first computer models applied to geologic problems. Briggs and Pollack (1967) developed the first digital simulation model accounting for flow and transport and precipitation of sea salt in order to test hypothetical paleogeographic configurations of a Paleozoic evaporite basin. Although from the present view their model appears to be strongly simplified, their work marks the beginning of quantitative sedimentation modeling methods. Without going into details of their model, principal drawbacks were the lack of geochemical considerations and the fact that water depth was not accounted for as a critical factor for flow and evaporite sedimentation. Another problem was that no mass balance calculation was performed in spite of the fact that the finite difference approach for the solution of the transport equation usually tends to damage mass balances at high Peclet numbers.

The SIMSAFADIM model (Bitzer and Salas, 2002), which has been applied in this study, is a 3D finite element model. It was initially designed for the simulation of carbonate sedimentation and has later been coupled with clastic sedimentation. The model provides a combination of well documented and tested algorithms for simulating flow and transport, adapted from Kinzelbach (1985), in combination with sedimentary processes, which are represented by a set of ordinary differential equations. Details of the sedimentation modeling are given in Bitzer and Salas (2001). In order to include evaporite sedimentation, several modifications have been incorporated regarding the simulation of evaporation outflow, transport of solutes and the precipitation process of solutes. Details of the evaporite model are given elsewhere. Flow is simu-

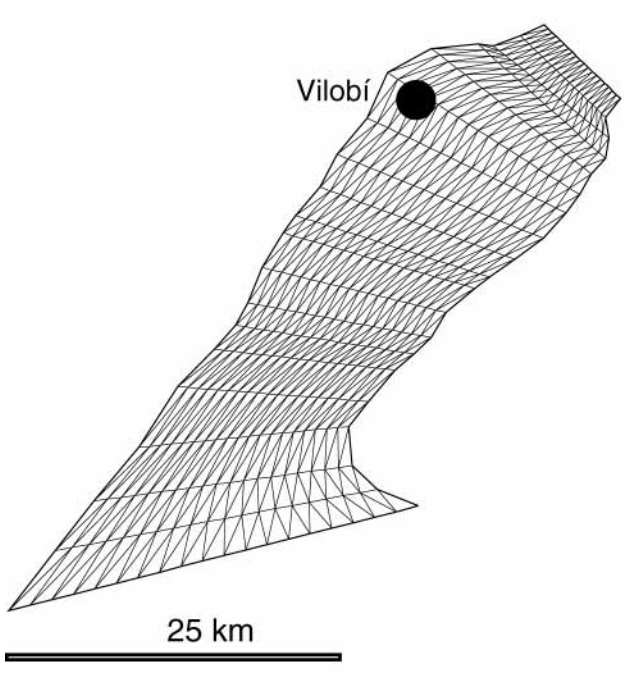

FIGURE 5 | **Finite element mesh of the upper Burdigalian Vallès-Penedès embayment used for simulation calculations.**

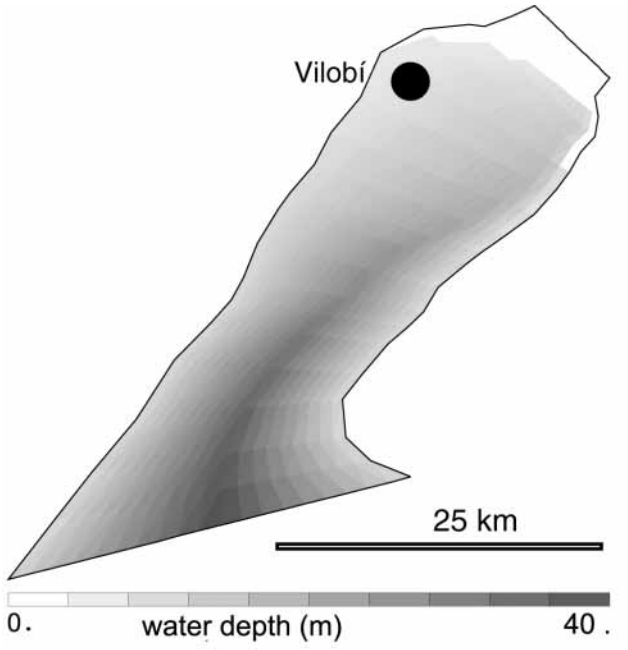

FIGURE 6 | **Initial water depth for fixed sea level simulation runs.**

lated as a 2D potential flow, thus density driven and wind driven flow components are not considered. Driving processes of flow in the basin are evaporation outflow, inflow of sea water and inflow of one or more freshwater sources. Flow depends on water depth, however flow direction and velocity do not vary with circulation depth.

The restriction to two dimensions in space is a major simplification which affects considerably simulated evaporite sedimentation rates and patterns. Simulated flow fields only represent surficial water flow. Flow velocities and directions at greater depth would be different from the simulated flow field.

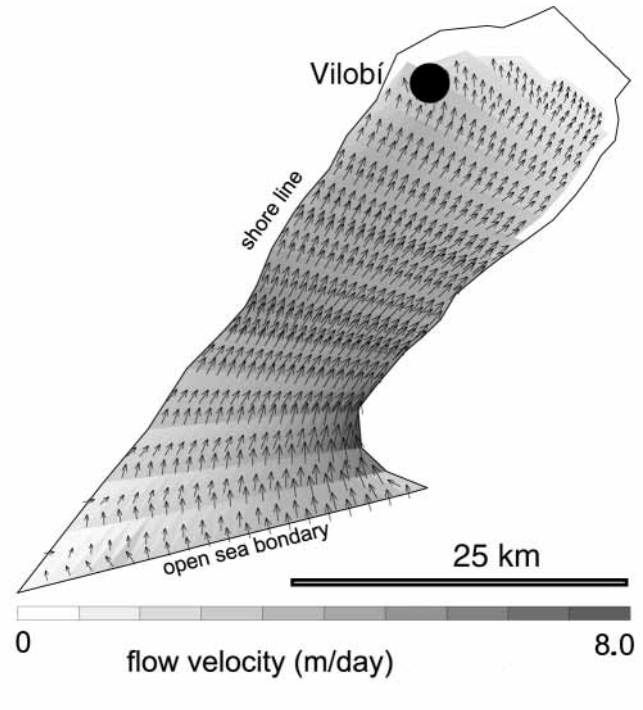

FIGURE 7 | **Flow field without freshwater inflow at river mouth.**

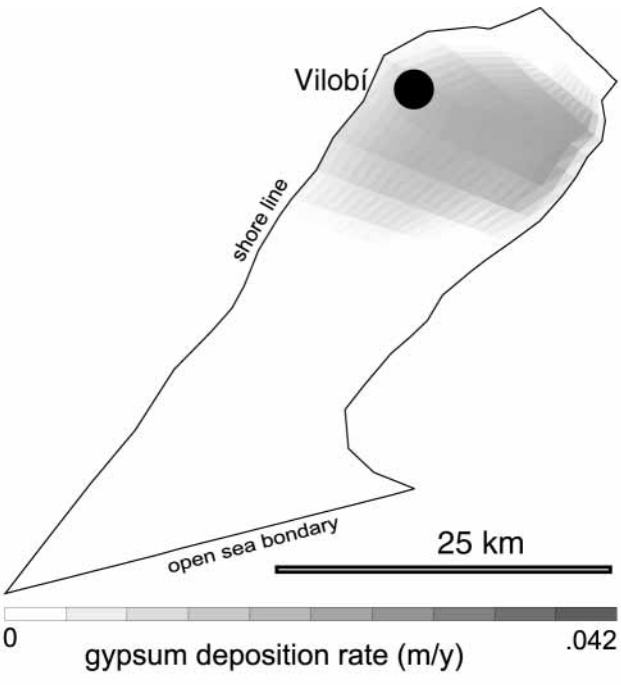

FIGURE 8 | **Gypsum deposition rates without freshwater inflow.**

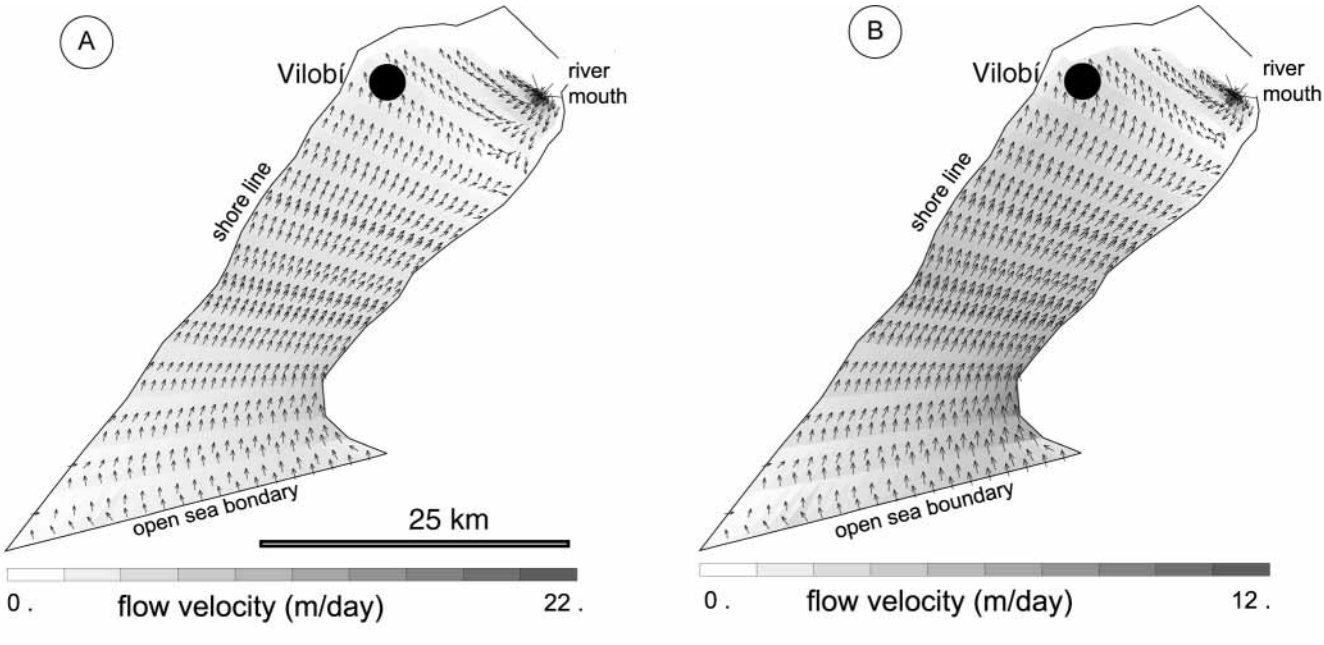

FIGURE 9 | **Flow field. A) With 2000 l/s freshwater inflow at river mouth. B) With 1000 l/s freshwater inflow at river mouth.**

MODEL PARAMETERS

Varying assumptions on paleogeographic, hydrological and climatic conditions of the upper Burdigalian basin configuration have been tested in different simulation runs. A possible estuarine river mouth at the northeastern termination of the upper Burdigalian Vallès-Penedès embayment, various freshwater discharge rates at the river mouth and different evaporation outflow rates have also been tested.

The possible configuration of the upper Burdigalian basin has been estimated from Guimerà et al. (1992), and water depth has been roughly estimated from facies data and sediment thickness. The triangular finite element mesh (Fig. 5) incorporates a total of 800 elements. Simulation time is 300 y for all calculations with steady state sea level. This time span is in all simulation runs sufficient to achieve steady state concentrations at the onset of gypsum precipitation for the given inflow and evaporation outflow rates. Evaporation outflow has been varied between 0.5 and 1.0 m/y, which appears to be a realistic range of values given the present day data from the western Mediterranean and modern analogues of evaporite deposition areas such as the Arabian Gulf. Discharge of freshwater at a hypothetical river mouth has been varied between 0 and 5000 l/s. Boundary conditions for flow are defined through areal evaporation outflow, river discharge rates to the bay and fixed potential at the open sea. Boundary conditions for transport are defined through zero solute concentration at the river mouth discharge and fixed concentrations at the open sea. Carbonate and clastic sedimentation have not been incorporated, as both are assumed to be of low importance for the formation of evaporite sediments, and in order to limit calculation time. Simulation runs with static and dynamic sea level have been performed. The presented simulation results may help to estimate conditions in the Vallès-Penedès basin during upper Burdigalian time.

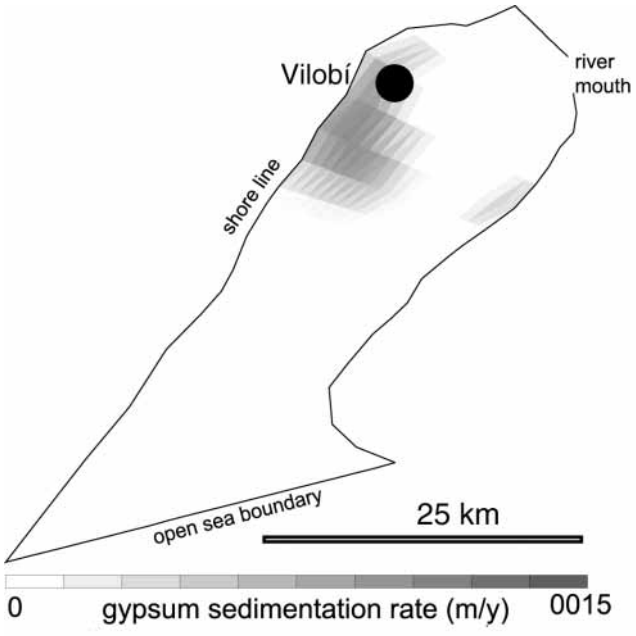

FIGURE 10 | **Gypsum deposition rates at 1000 l/s freshwater inflow.**

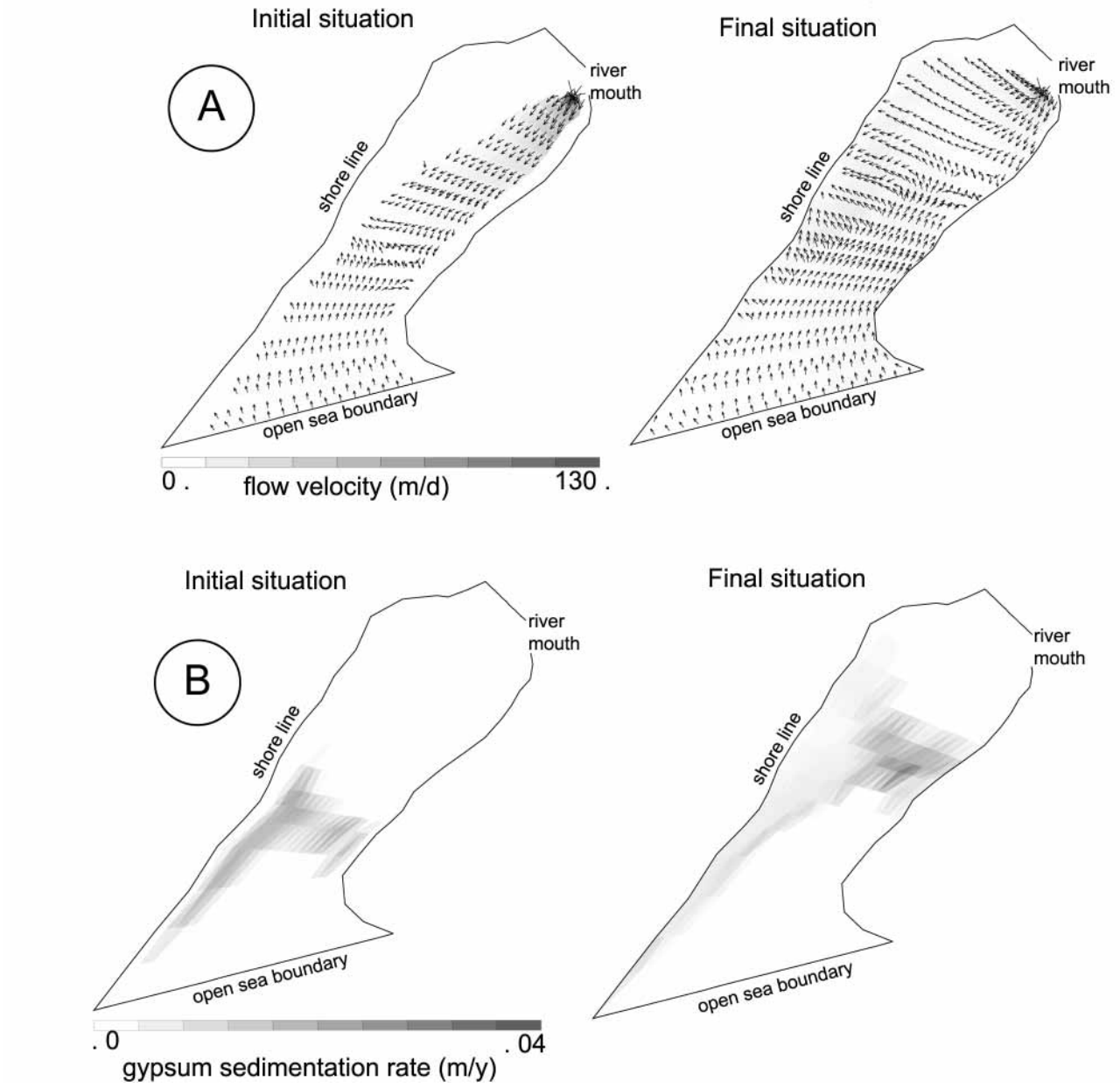

FIGURE 11 **A) Initial and final flow field with dynamic sea level simulation runs. B) Initial and final gypsum deposition rate with dynamic sea level simulation runs.**

RESULTS

Basin configuration for simulation runs with fixed sea level shows initial water depth of 40 m at the open sea boundary, smoothly shallowing towards the shore line (Fig. 6). White areas within the limits of the finite element mesh indicate water depth below 0.5 m. A river mouth is assumed in the northeastern prolongation of the bay. Discharge rates have been varied between 0 and 5000 l/s. Simulation time in fixed sea level simulation runs has been limited to 300 years, as this time span is sufficient to establish a steady state system.

Figure 7 shows the simulated flow field for an evaporation outflow rate of 1 m/y, without any freshwater inflow. The flow field shows inflow from the open sea with maximum flow velocities reaching up to 8 m/day. Gypsum precipitation is calculated for the northern shoreline of the bay (Fig. 8). As should be expected, the simulation run predicts increasing evaporite deposition in most parts of the considered basin zone.

Setting freshwater inflow to 2000 l/s at the river mouth at an evaporation outflow of 1 m/y shows a complex flow field with freshwater flow from the river mouth and sea water inflow from the open ocean due to evaporation in the bay (Fig. 9A). The freshwater discharge at the river mouth prevents gypsum precipitation in the northern part of the bay. Gypsum precipitation is calculated in those parts of the basin where freshwater influence ends due to evaporation outflow.

At an evaporation outflow of 1 m/y and reduced freshwater inflow of 1000 l/s, the simulated flow field again exhibits two converging flow systems, which meet in the upper part of the basin (Fig. 9B). Freshwater flows from the river mouth towards south into the bay and mixes with sea water flowing from the open sea. Gypsum saturation would be reached in some parts of the basin, and gypsum precipitation rates up to 0.0015 m/y are calculated mainly along the western shore line (Fig. 10). Within a small area at the opposite shore line, some gypsum deposition is calculated as well. Freshwater inflow, evaporation outflow and geometric configuration of the basin create a complex flow field with conditions which might provide gypsum deposition.

Calculations with dynamic sea level were performed in order to test the possible relation between deposition of evaporites and a transgressive pulse. Initial sea level is 10 m lower than in examples 1-4 and rises 10 m during the simulation run which extends 3000 years, such that the final situation coincides with sea level position of the fixed sea level simulation runs. A river discharge is defined with 5000 l/s. Figure 11A shows the flow field, which has initially a much smaller extension due to the sea level lowstand. At the end of the calculation, sea level has risen and the basin is completely flooded, showing a complex flow pattern imposed by freshwater discharge, basin geometry and bathymetry. Flow velocity is elevated due to increased freshwater inflow and reaches maximum velocities of 130 m/day at the river mouth. The mixing zone between freshwater and sea water is displaced towards the open sea, which is the principal reason for evaporite sedimentation being calculated at the more southward zones compared to the previous example (Fig. 11B). Due to the transgression, continued flooding towards the north is accompained by gypsum precipitation, with maximum deposition rates reaching up to 0.04 m/y, which appears to be unrealistic high.

CONCLUSIONS

Without any freshwater discharge from a hypothetic river mouth, evaporation outflow provokes evaporite deposition in the basin regardless of evaporation outflow rates. Evaporite sedimentation starts in those zones which are most distant to the open sea and extends continously to peripherical zones as evaporation outflow continues, until a steady state system is achieved. Freshwater inflow displaces the zone of evaporite deposition towards the open sea, and the rate of freshwater inflow controls the extent of this displacement. However, if freshwater inflow is too high, the dilution process dominates and evaporites may not form anywhere in the bay. The controlling factor for the evolution of evaporite sediments in the basin appears to be the freshwater supply into the basin. Simulation runs with fixed sea level indicate that for the chosen geometry and topography of the upper Burdigalian Penedès basin, the freshwater inflow should have been above 2000 l/s at an evaporation rate of 1 m/y in order to prevent gypsum deposition in most parts of the basin. Calculations involving dynamic sea level predict that evaporite sediments should also be expected during the early transgressive pulse in the more southward located parts of the basin, if freshwater inflow was less than 5000 l/s.

In order to explain the absence of marine evaporites in the basin during the transgressive phase during upper Burdigalian embayment, hydrological conditions appear to be the principal factor for preventing gypsum precipitation. Simulation runs show that even very low freshwater inflow rates in the order of 2000 l/s are sufficient to prevent concentration of brines sufficient to precipitate gypsum in most parts of the upper Burdigalian Penedès basin at evaporation outflow of 1 m/y. The Vilobí Gypsum sequence appears to be a deposit, where sabkha-salina evaporite facies have been possible due to

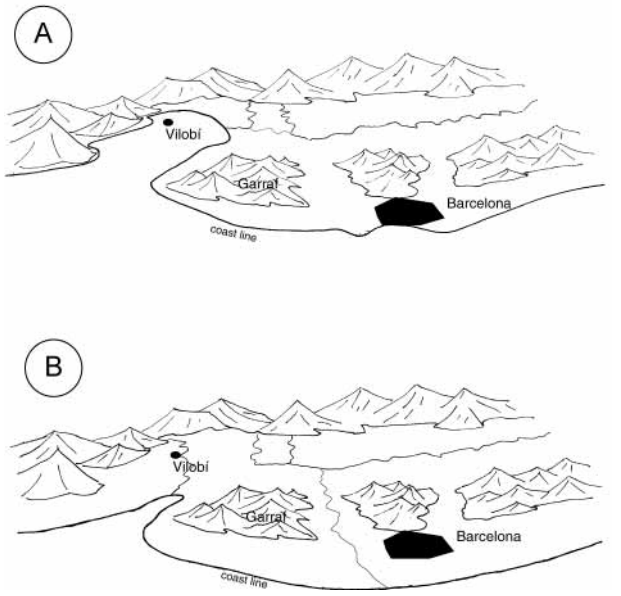

FIGURE 12 **A) Schematic paleogeographic configuration and basin drainage system in the southern Vallès-Penedès half-graben. A) During the upper Burdigalian transgressive pulse. B) After the upper Burdigalian.**

the fact, that it may have been a zone sufficiently isolated from any significant freshwater (diffuse groundwater and river) inflow. The following flooding of the basin was accompanied by a mixing of marine water and freshwater in the whole basin, preventing any evaporite deposition.

Freshwater availability in the basin may have changed during the Neogene evolution of the basin. The present day fluvial system of the Vallès-Penedès basin shows a surface water drainage principally towards the Barcelona area (Fig. 1). The paleogeographical maps shown in Guimerà et al. (1992) and Roca et al. (1999), however, indicate a fluvial system which has probably been different from the present system. A river drainage along the complete basin axis with discharge in the western area may have provided a high freshwater discharge in the western termination of the basin (Fig. 12A). The absence of marine evaporite sediments in the Penedès basin may be interpreted in that way, that the Llobregat and Besós river breakthrough at Barcelona happened at later stages, affecting freshwater and sediment supply in the basin when the marine episode in the Penedès basin was already over (Fig. 12B).

ACKNOWLEDGEMENTS

I am deeply grateful to Francesc Calvet who showed me the Vallès-Penedès basin on various fieldtrips and who made this visit an extremely fortunate and rewarding experience for me. Thanks are given to Federico Ortí (Universitat de Barcelona) for valuable discussions regarding details of the sedimentary column of the Vilobí sequence. I strongly benefitted from comments by Carlos Ayora (Institut Jaume Almera, CSIC, Barcelona). Winfried Gade (Universität Bayreuth) performed calculations on solubility of gypsum using PHREEQ-C. Thanks to Ramon Salas (Universitat de Barcelona) for colaboration with the SIMSAFADIM model and Christiana Scharfenberg for correcting the original manuscript. This work was partly supported by the Instituto Mexicano del Petroleo (IMP). Some parts of this work date back to my visit in the Departament de Geoquímica, Petrología I Prospecció Geològica at the Facultat de Geología at the Universitat de Barcelona from 1994 to 2000.

REFERENCES

Alsharhan, A.S., Kendall, C.G.St.C., 2003. Holocene coastal carbonates and evaporites of the southern Arabian Gulf and their ancient analogues. Earth-Science Reviews, 61, 191-243.

Ayora, C., García Veigas, J., Pueyo, J.J., 1994. The chemical and hydrological evolution of an ancient potash-forming evaporite basin as constrained by mineral sequence, fluid inclusion, and numerical modeling. Geochimica et Cosmochimica, 16, 3379-3394.

Bethke, C.M.,1996. Geochemical reaction modeling. New York, Oxford University Press, 397 pp.

Bitzer, K., Salas, R., 2001. Simulating carbonate and mixed carbonate-clastic sedimentation using predator-prey models. In: Merriam, D., Davies, J., (eds.). Geologic modeling and simulation: Sedimentary Systems. Amsterdam, ed. Kluwer Academic Publishers Co., 169-204.

Bitzer, K., Salas, R., 2002. SIMSAFADIM: 3D simulation of stratigraphic architecture and facies distribution modeling of carbonate sediments. Computers & Geosciences, 28, 1177-1192.

Briggs, L.I. , Pollack, H.N.,1967. Digital model of evaporite sedimentation. Science, 155, 453-456.

Cabrera, L., 1981. Estratigrafía y características sedimentológicas generales de las formaciones continentales del Mioceno inferior de la cuenca del Vallès-Penedès (Barcelona, España). Estudios geológicos, 37, 35-43.

Cabrera, L., 1982. Influencia de la tectónica en la sedimentatción continental de la cuenca del Vallès-Penedès (provincia de Barcelona) durante el Mioceno inferior. Acta Geologica Hispanica, 16, 163-169.

Cabrera, L., Calvet, F., Guimerà, J., Permanyer, A., 1991. El registro sedimentario miocenico en los semigrabens del Vallès-Penedès y el Camp: organización secuencial y relaciones tectónica sedimentación. Libro-Guía Excursión nº 4, I Congreso del grupo Español del Terciario, Vic 1991, 132 pp.

Custodio, E., Bruggeman, G.A., Cotecchia, V., 1987. Groundwater problems in coastal areas. Paris, UNESCO, Studies and Reports in Hydrology, 35, 241 pp.

Dietrich, G., 1959. Ozeanographie. Braunschweig, ed. Westermann Verlag , 118 pp.

Eugster, H.P., Hardie, L.A., 1978. Saline lakes. In: Lerman, A. (ed.). Lakes: Chemistry, Geology, Physics. New York, Springer, 237-293.

Gratacós, O., Bitzer, K., Cabrera, L., Roca, E., Salas, R., 2003. 3D simulation of sedimentary facies: application to oil bearing Langhian reef buildups in the Vallès -Penedès basin (Catalunya, Spain). Annual AAPG conference, Barcelona, 22.9.-26.9.2003.

Guimerà, J., Anadón, P., Cabrera, L., Estévez, A., Fontboté, J.M., Fornós, J., Martí, J., Mató, E., Muñoz, J.A., Pomar, L., Pueyo, J.J., Puigdefábregas, C., Ramos, E., Riba, O., Roca, E., Rodríguez-Perea, A., Sàbat, F., Sáez, A., Santanach, P., Saula, E., Soria, J., Taberner, C., Vergés, J., 1992. Història Natural dels Països Catalans. Geologia (II). Barcelona, Fundació Enciclopedia Catalana, 548 pp.

James, A.N., 1992. Soluble materials in civil engineering. New York, Ellis Horwood Publications Co., 434 pp.

Kinsman, D.J.J., 1976. Evaporites: relative humidity control of primary mineral facies. Journal of Sedimentary Petrology, 46, 273-270.

Kinzelbach, W., 1985. Groundwater modeling: an introduction with sample programs in BASIC. Amsterdam, ed. Elsevier, 331 pp.

Ortí, F., 1990. Yesos de Vilobí (Mioceno). In: Ortí, F., Salvany, J. M. (eds.). Formaciones evaporíticas de la cuenca del Ebro y cadenas periféricas, y de Levante. Barcelona, ENRESA, 306 pp.

Ortí, F., Pueyo, J.J., 1976. Yeso primario y secundario del depósito de Vilobí (provincia de Barcelona, España). Instituto de Investigaciones Geológicas, 31, 5-34.

Risacher, F., Clement, A., 2001. A computer program for the simulation of evaporation of natural waters to high concentration. Computers & Geosciences, 27, 191-201.

Roca, E., Sans, M., Cabrera, L., Marzo, M., 1999. Oligocene to Middle Miocene evolution of the central Catalan margin (northwestern Mediterraean). Tectonophysics, 315, 209-233.

Tolmazin, D., 1985. Elements of dynamic oceanography. London, ed. Allen & Unwin, 181 pp.

Turekian, K.K., 1985. Die Ozeane. Stuttgart, ed. Enke Verlag, 202 pp.

Voigt, H.J., 1990. Hydrogeochemie. Berlin, ed. Springer, 310 pp.

Yechieli, Y., Wood, W.W., 2002. Hydrogeologic processes in saline systems: playas, sabkhas and saline lakes. Earth-Science Reviews, 58, 343-365.

Manuscript received October 2003;
revision accepted June 2004.